TISSUE ENGINEERING: Part A
Volume 22, Numbers 9 and 10, 2016

DOI: 10.1089/ten.tea.2015.0536

termis
Tissue Engineering
& Regenerative Medicine
International Society

ORIGINAL ARTICLE

Cellularized Bilayer Pullulan-Gelatin Hydrogel for Skin Regeneration

Mathew N. Nicholas, BMSc, Marc G. Jeschke, MD, PhD, FACS, FCCM, FRSC(C), and Saeid Amini-Nik, MSc, MD, PhD

Skin substitutes significantly reduce the morbidity and mortality of patients with burn injuries and chronic wounds. However, current skin substitutes have disadvantages related to high costs and inadequate skin regeneration due to highly inflammatory wounds. Thus, new skin substitutes are needed. By combining two polymers, pullulan, an inexpensive polysaccharide with antioxidant properties, and gelatin, a derivative of collagen with high water absorbency, we created a novel inexpensive hydrogel—named PG-1 for ''pullulan-gelatin first generation hydrogel''—suitable for skin substitutes. After incorporating human fibroblasts and keratinocytes onto PG-1 using centrifugation over 5 days, we created a cellularized bilayer skin substitute. Cellularized PG-1 was compared to acellular PG-1 and no hydrogel (control) *in vivo* in a mouse excisional skin biopsy model using newly developed dome inserts to house the skin substitutes and prevent mouse skin contraction during wound healing. PG-1 had an average pore size of 61.69 μm with an ideal elastic modulus, swelling behavior, and biodegradability for use as a hydrogel for skin substitutes. Excellent skin cell viability, proliferation, differentiation, and morphology were visualized through live/dead assays, 5-bromo-2′-deoxyuridine proliferation assays, and confocal microscopy. Trichrome and immunohistochemical staining of excisional wounds treated with the cellularized skin substitute revealed thicker newly formed skin with a higher proportion of actively proliferating cells and incorporation of human cells compared to acellular PG-1 or control. Excisional wounds treated with acellular or cellularized hydrogels showed significantly less macrophage infiltration and increased angiogenesis 14 days post skin biopsy compared to control. These results show that PG-1 has ideal mechanical characteristics and allows ideal cellular characteristics. *In vivo* evidence suggests that cellularized PG-1 promotes skin regeneration and may help promote wound healing in highly inflammatory wounds, such as burns and chronic wounds.

Introduction

Currently, skin substitutes are extensively used in treating both burns and chronic skin wounds.[1,2] These skin substitutes have significantly decreased morbidity and mortality of these injuries, yet there are still a number of challenges skin substitutes face.[3] These include complications due to highly inflammatory wounds, poor skin regeneration, and high costs.[1,3–5] This leads to adverse events causing potential death, poor aesthetic and functional outcomes, and expensive treatments. Thus, further research into the creation of skin substitutes that solve these challenges is needed.

Currently, the two main components of a skin substitute consist of the three-dimensional porous structure known as the hydrogel and the cells incorporated into it. The hydrogel of a skin substitute heavily depends on the compounds from which it is created.[6] Pullulan is a relatively inexpensive polysaccharide only recently being used in hydrogels.[7] The compound is nontoxic, nonimmunogenic and nonmutagenic, and has good antioxidant potential.[7,8] These properties have shown that pullulan is an ideal compound for use in skin substitutes and can both be incorporated with and recruit viable skin cells.[8,9] On the other hand, gelatin is an irreversibly hydrolyzed form of collagen that has been used extensively in hydrogels.[6] Gelatin by itself is not often used in skin substitutes due to its unfavorable effects on cellular and mechanical properties.[10,11] Yet, it is commonly combined with other compounds as it has an ability to absorb relatively large quantities of water, a crucial component of skin substitutes.[12] In this study, we combine these two compounds using a solvent casting-particulate leaching followed by subsequent freeze-drying methodology. The use of these two methods in combination allows for a quick and simple production of hydrogels to create highly porous structures consisting of inexpensive materials that can be custom-developed for shaping.[13]

Although there are a number of acellular skin substitutes available, there is a large amount of evidence that highlights

Department of Surgery, Sunnybrook Research Institute, Ross Tilley Burn Centre, University of Toronto, Toronto, Ontario, Canada.

the benefits of cellularized skin substitutes for skin regeneration.[14] The predominant cell lines found in human skin consist of fibroblasts, which make up most of the dermal layer, and keratinocytes, which make up most of the epidermal layer. There is mounting evidence that incorporating both fibroblasts and keratinocytes into skin substitutes significantly increases skin regeneration due to positive cross-talk between these cell lines.[15–17] This study uses this knowledge to create cellularized bilayer skin substitutes using a novel methodology involving centrifugation over a 5-day period to maximize skin regeneration potential.

Here, we used pullulan and gelatin to create a hydrogel—hereafter named PG-1 for ''pullulan-gelatin first generation hydrogel''—ideal for skin substitutes. We incorporated human fibroblasts and keratinocytes *in vitro* to create bilayer skin substitutes to improve wound healing and skin regeneration in a mouse skin punch biopsy. This novel skin substitute shows optimal mechanical characteristics and superior cellular characteristics, which translate into significantly increased wound healing and decreased inflammation.

Materials and Methods

Human skin samples

Normal human skin samples were obtained from healthy men and women aged 40–60 years undergoing various plastic surgeries at Sunnybrook Health Sciences Centre, University of Toronto, Toronto, ON, Canada. Tissue specimens were obtained with patient-signed informed consent according to the Declaration of Helsinki Principles, following Toronto Academic Health Sciences Network (TAHSN) and University of Toronto-affiliated Sunnybrook Research Institute and Sunnybrook Health Sciences Centre Institutional Ethics Review Board approval.

Cell culture

Primary human normal skin fibroblasts and human epithelial keratinocytes were obtained from skin tissue samples. Tissue culture materials were purchased from BD Falcon™, and all tissue culture media and supplements were obtained from Wisent, Inc., unless otherwise stated. Primary keratinocytes were isolated using the protocol described by Aasen and Izpisúa Belmonte.[18] Primary fibroblast cultures were isolated by first dissecting human skin to remove adipose tissue and cutting the skin into explant pieces of 2–4 mm. Explants were cultured in Petri dishes for 7 days before further passaging. When fibroblasts reached 70% confluence ($\sim$5 days), they were trypsinized with 0.05% trypsin/0.025% ethylenediamine tetraacetic acid v/v in preparation for subculture.

After isolation of each cell line, fibroblasts and keratinocytes were subcultured in 75 cm^2 tissue culture flasks until 70% confluence was reached. Fibroblasts were grown in high-glucose Dulbecco's modified Eagle's medium supplemented with 10% fetal bovine serum and 1% antibiotic-antimycotic solution. Keratinocytes were grown in EpiLife® medium supplemented with human keratinocyte growth supplement from Cascade Biologics and 1% antibiotic-antimycotic solution. Media was changed every 48–72 h. Collected tissues and cells were cultured at 37°C in a humidified atmosphere with 5% carbon dioxide. Cells were frozen overnight in 90% phosphate-buffered saline (PBS) and 10% dimethyl sulfoxide from Sigma-Aldrich® solution at −80°C in a Mr. Frosty™ Freezing Container from Thermo Scientific and then stored in liquid nitrogen until incorporated into PG-1.

Creation of pullulan-gelatin hydrogel

PG-1s were created using a solvent casting-particulate leaching and freeze-drying methodology. About 1.68 g of pullulan (Sigma-Aldrich) and 0.42 g of gelatin from BioShop® were dissolved in 4.5 mL of ddH_2O. Eighteen grams of powdered sodium chloride (BioShop) were extensively mixed into the solution. 0.3 g of trisodium trimetaphosphate (Sigma-Aldrich) was mixed with 0.3 mL 10 M sodium hydroxide solution (BioShop), combined with the pullulan solution, and poured into an 8×8 cm square plate with a 1.6 mm thickness. An 8×8 cm glass plate was placed on top to compress the solution. The plated solution was incubated for 45 min at 50°C under negative vacuum pressure. The resulting solid sheet was removed and underwent three PBS washes followed by 10%, 20%, and 30% ethanol washes. Eight millimeter punch biopsies were taken from the sheet and frozen at −80°C for 2 h. The frozen hydrogels were then placed in a Lyph-Lock 4.5 freeze-dryer from Labconco overnight under negative pressure and at −40°C.

Incorporation of cells into pullulan-gelatin hydrogel

Dry PG-1s were placed in a 48-well plate and sterilized by ultraviolet light for at least 30 min. Both fibroblasts and keratinocytes were thawed and grown separately in a 75 cm^2 tissue culture flask until 70% confluence before incorporation into PG-1. At time of incoporation, only fibroblasts with a passage of 15 or less and keratinocytes with a passage of 7 or less were used. Fibroblasts were added by placing a 10 μL drop of fibroblast media with 50,000 fibroblasts on the surface of the hydrogel. The hydrogels were centrifuged at 50 g for 10 min and then flipped over. Similar drops of fibroblasts were added to the other side of the hydrogels followed by further centrifugation. The hydrogels were incubated in 1 mL of fibroblast medium for 48 h and then the medium was discarded.

Before adding keratinocytes, in order to increase keratinocyte adherence thus increasing the number of keratinocyte clusters, 1 μL of laminin from Engelbreth-Holm-Swarm murine sarcoma basement membrane (Sigma-Aldrich) was added dropwise to the top surface of each hydrogel followed by a 2-h incubation. Laminin was used as it is a crucial component of human skin basement membrane and the use of laminin is known to increase basal keratinocyte adherence and migration.[19] About 100,000 keratinocytes in a 10 μL drop of keratinocyte media were seeded dropwise on to the surface of the hydrogel. Following brief centrifugation, hydrogels were incubated in 1 mL of keratinocyte media for 72 h and subsequently prepared for confocal imaging or *in vivo* use. Although other methodologies for incorporating cells into skin substitutes have been published and compared,[20] this modified centrifugation provided the most customizable method in creating a skin substitute with two cell layers without destroying the hydrogel's native architecture.

Mechanical Characteristics

Porosity

Dry hydrogels were imaged with a Hitachi S-3400N scanning electron microscopy at the University of Toronto,

Toronto, ON, Canada after being gold sputter coated. Images were then analyzed using ImageJ software (National Institutes of Health). Porosity was obtained by measuring two diameters perpendicular to each other of all pores in view in representative images from three different hydrogels.

In vitro *degradation*

In vitro enzymatic degradation was evaluated by taking dry hydrogels ($n = 5$) and incubating them in 1 mL of PBS at 37°C in a humidified atmosphere with 5% carbon dioxide. Hydrogels were weighed and placed in 1 mL of pullulanase microbial (Sigma-Aldrich) and incubated in similar conditions. Hydrogels were weighed every 5 min until they were unable to be manipulated and weighed due to degradation.

Swelling behavior

Dry hydrogels were weighed and then sterilized under ultraviolet light for at least 30 min. Hydrogels ($n = 5$) were placed in 1 mL of PBS, fibroblast growth media, or keratinocyte growth media for 24 h and incubated at 37°C in a humidified atmosphere with 5% carbon dioxide. The wet hydrogels were gently wiped with a Kimwipe® and weighed. Their swollen weight (m_s) was compared to their dry weight (m_d) to obtain their swelling percentage using the equation: Swelling (%) $= [(m_s - m_d)/m_d] \times 100\%$.

Elastic modulus

Elastic modulus was tested on 2×1 cm rectangles ($n = 6$) of hydrogel material using an 840 Family Compact Electrodynamic Fatigue Test at the University of Toronto, Toronto, ON, Canada. Rectangular hydrogels were soaked in 1 mL of PBS for 1 h before testing elastic modulus.

Cellular Characteristics

Live/dead assay

Live/dead assay was performed using a Live/Dead® Viability/Cytotoxicity Kit (Life Technologies®) on human fibroblasts and keratinocytes adhered onto different hydrogels at 5- and 3-day post-seed respectively to mimic cell viability at time of *in vivo* use. Imaging was performed on a Zeiss observer Z1 spinning disc confocal microscope (Zeiss). Quantification of viability was performed by counting the number of ethidium homodimer-1 negative cells compared to the total number of cells using ImageJ software. Data are presented as mean ± standard error of the mean (SEM) using three representative images of three different hydrogels.

5-Bromo-2′-deoxyuridine proliferation assay

5-Bromo-2′-deoxyuridine (BrdU) proliferation assay was performed by incubating hydrogels incorporated with either fibroblasts or keratinocytes in a 10 μL BrdU and 1 mL growth media solution for 24 h. The cellularized hydrogels were imaged using the Life Technologies BrdU Labeling and Detection Protocol. Quantification of viability was performed by counting the number of BrdU-positive cells compared to the total number of cells using ImageJ software. Data are presented as mean ± SEM using three representative images of three different hydrogels.

Immunofluorescence

Cellularized hydrogels were washed with PBS and fixed for 30 min in 4% paraformaldehyde (Alfa Aesar). Fixed hydrogels were washed in cold PBS and permeabilized for 10 min with PBS/0.5% Triton X-100 (Sigma-Aldrich) solution. After

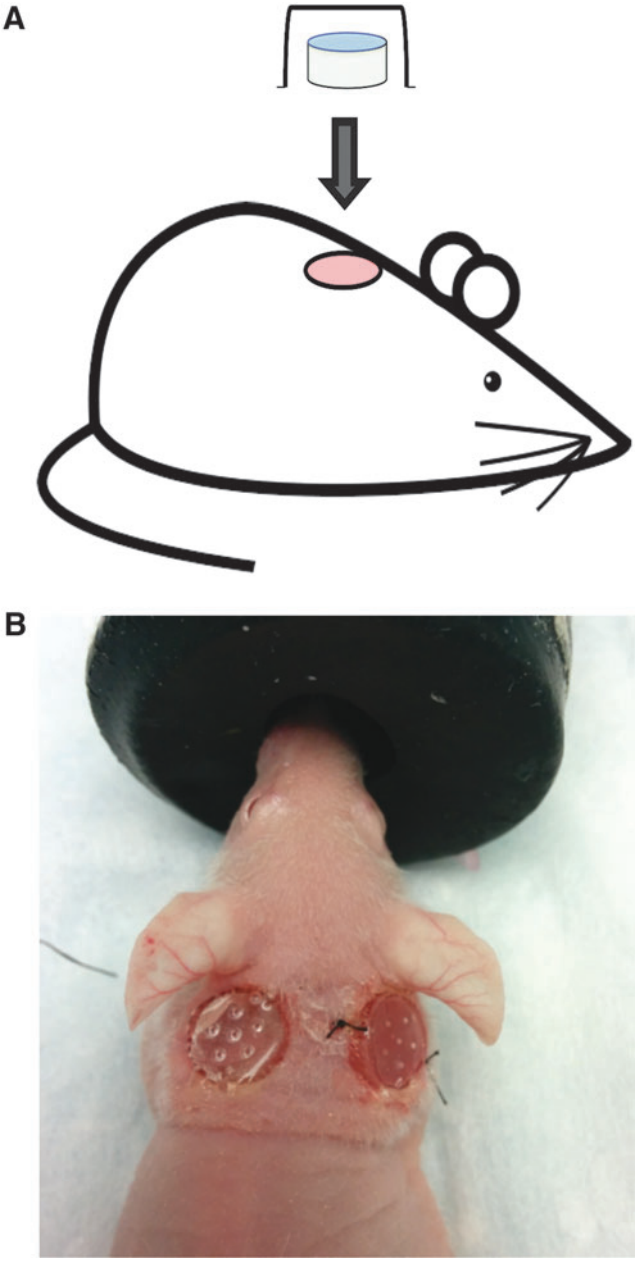

FIG. 1. Surgical model using bilayer cellularized PG-1. Schematic drawing **(A)** and representative image **(B)** of mouse model where two 6 mm diameter mouse skin punch biopsies were created on the back of immunosuppressed mice and skin substitutes were held in place on the wound using newly developed plastic domes. Animal wounds were randomly divided into three groups: control (no hydrogel), acellular hydrogel (hydrogel without cells), and cellularized hydrogel (bilayer hydrogel). The figure above shows the dome held in place using tissue glue (*left*) and nylon suture (*right*). In this experiment, domes were only secured with tissue glue. Color images available online at www.liebertpub.com/tea

washing in PBS, hydrogels were blocked for 30 min with 1% bovine serum albumin (BioShop) in PBS/0.5% Triton X-100 solution. A primary antibody was added and incubated overnight at 4°C. The primary antibodies used in this study included phalloidin conjugated with FITC (1:30; Invitrogen), monoclonal goat K14 antibody (1:100; Santa Cruz), monoclonal rabbit K10 antibody (1:400; Covance), and monoclonal rabbit E-Cadherin antibody (1:500; Novus).

After washing thoroughly with PBS, the corresponding secondary antibody was added to a 1% bovine serum albumin in PBS/0.5% Triton X-100 solution and incubated for 1 h at room temperature in the dark. Secondary antibodies used in this study included 488 donkey anti-goat antibody (1:500; Alexa Fluor®), 546 donkey anti-rabbit antibody (1:500; Alexa Fluor), and 546 donkey anti-rabbit antibody (1:500; Alexa Fluor). Hydrogels were washed three times in PBS and kept in PBS and 1:5000 4′,6-diamidino-2-phenylindole (DAPI). Hydrogels were examined and photographed on a Zeiss observer Z1 spinning disc confocal microscope. Three representative images were taken per hydrogel and three hydrogels were imaged for quantitative analysis.

In Vivo Experiments

Wound healing model

Fifteen J:Nu mice (8-week-old, male, body weight 19.4–27.7 g), a strain of nude immunodeficient mice, were obtained from Jackson Laboratory under the guidelines of the Sunnybrook Research Institute and Sunnybrook Health Sciences Animal Policy and Welfare Committee of the University of Toronto. Animal procedures were reviewed and approved by Sunnybrook Research Institute and Sunnybrook Health Sciences Centre at University of Toronto Animal Care and Use Committee. Animals were anesthetized and two pairs of 6 mm diameter full-thickness wounds were created on the back of the mouse on either side from the midline (Fig. 1). Animal wounds were randomly divided into three groups: control (no hydrogel), acellular hydrogel (hydrogel without cells), and cellularized hydrogel (bilayer hydrogel). Each group consisted of five wounds on the left side and five wounds on the right side of the midline.

To prevent skin contraction, each wound used a newly developed plastic 8 mm dome insert 3D-printed specifically for this wound healing study, which was held in place using tissue glue. The use of a dome larger than the wound size allowed the mouse skin to stretch and secure itself to the dome. Hydrogels 8 mm in diameter were used to fit inside the dome. Each wound was observed twice a day until 14 days post skin biopsy. The mice were euthanized and their wounds were excised along with 2 mm of satellite skin to be sent for further histologic analysis. Only wounds that continued to have their dome intact until the end time point were used for analysis (control—$n=7$, acellular—$n=7$, cellular—$n=5$). Due to the opaque material of each dome, it was not possible to take pictures of healing wounds at various time points.

Trichrome staining

Trichrome reagents were obtained from EMS unless otherwise stated. Paraffin-embedded slides of excised wounds

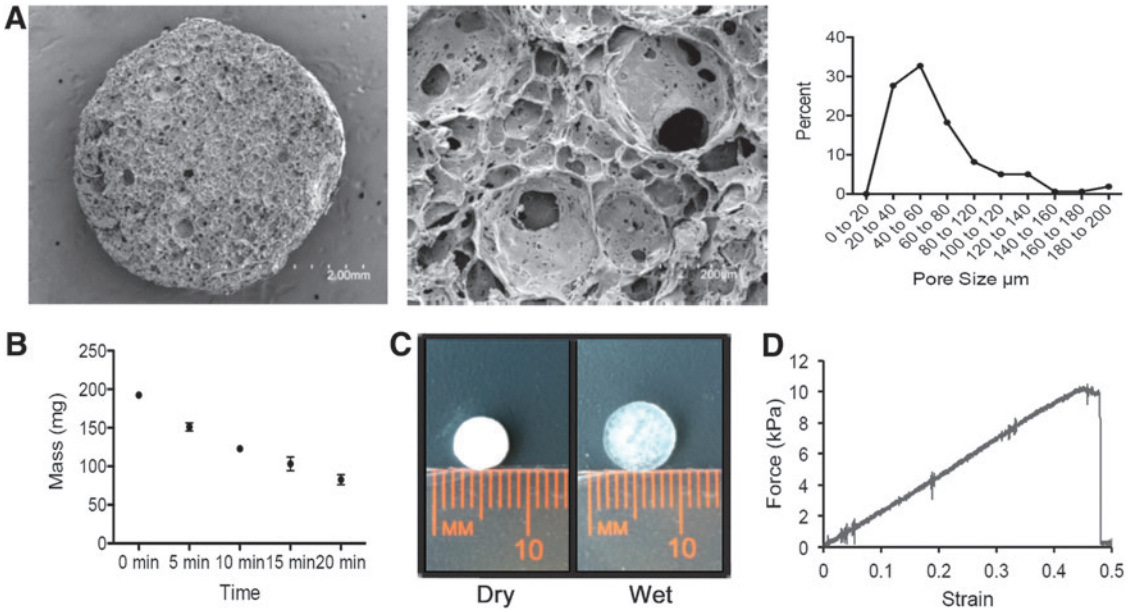

FIG. 2. Mechanical characteristics of PG-1. **(A)** Scanning electron microscopic images of pullulan-gelatin hydrogel at 27× magnification (*left panel*) and 75× magnification (*center panel*). Images at 75× magnification were used to quantify pore sizes. Pore size distribution was plotted (*right panel*). Average pore size was 61.69 ± 2.76 µm (mean ± SEM) with a range of pore sizes from 20 to 200 µm. **(B)** The mass of PG-1 over time when submerged in pullulanase microbial is shown. Hydrogels could no longer be placed on a scale after 20 min due to significant degradation. **(C)** Image shows increase in hydrogel size after being incubated in PBS. Swelling percentage of pullulan-gelatin hydrogel ranged from 1812% ± 25.46%, 1758% ± 31.74%, and 1801% ± 43.49% (mean ± SEM) when incubated in PBS, fibroblast media, and keratinocyte media respectively. **(D)** Sample stress-strain curve for PG-1 is shown. Elastic modulus of the pullulan-gelatin material was 22.43 ± 4.54 kPa (mean ± SEM). PBS, phosphate-buffered saline; SEM, standard error of the mean. Color images available online at www.liebertpub.com/tea

were heated at 60°C for 30 min and then deparaffinized with citrosol washes and rehydrated through 100%, 95%, and 70% alcohol washes. Following a wash in distilled water, slides were refixed in Bouin's solution (26367-01) for 1 h at 56°C. Slides underwent a wash in running tap water and were stained in Weigert's iron hematoxylin working solution (Sigma-Aldrich) for 10 min. After a wash in distilled water, slides were stained in Biebrich scarlet-acid fuchsin for 10 min and washed again in distilled water. Slides were then differentiated in phosphomolybdic-phosphotungstic acid solution for 15 min and transferred directly into an aniline blue solution stain for 5 min. Next, slides were briefly rinsed in distilled water, differentiated in 1% acetic acid solution for 2 min, and washed once more in distilled water. The slides were then dehydrated quickly using 95% and 100% alcohol and cleared in citrosol. Slides were mounted on a coverslip using xylene-based mounting medium (Triangle Biomedical Sciences).

Immunohistochemistry

Paraffin-embedded slides of excised wounds were heated at 60°C for 30 min and then deparaffinized with citrosol washes and rehydrated through 100%, 95%, and 70% alcohol washes. Then, 1× antigen decloaker solution (Biocare Medical) was preheated in a decloaking chamber at 70°C for 20 min before the hydrated slides were added. The solution and slides were heated at 110°C for 4 min, cooled to 50°C, and then washed with water. Wounds were circled with a hydrophobic pen on the slides and blocked with 3% H_2O_2 for 10 min. Following a wash with washing buffer (0.05 M Tris-HCl, 0.15 M NaCl, and 0.05% Tween 20 in deionized water), slides were incubated with a primary antibody in PBS for 1 h at room temperature. Primary antibodies used include mouse monoclonal human leukocyte antigen (HLA) class 1 antibody (1:100; Abcam), rat monoclonal F4/80 antibody (1:200; AbD Serotec), mouse monoclonal proliferating cell nuclear antigen (PCNA) antibody (1:2000; Cell Signaling), and rabbit monoclonal alpha-smooth muscle antibody (ASM) (1:200; Abcam).

Slides were washed with washing buffer and then the MACH3 probe (Biocare Medical) corresponding to the appropriate antibody species was added for 15 min. Slides were washed again with washing buffer and the species-appropriate MACH3 horseradish peroxidase polymer detection was added for 15 min. Following another wash with washing buffer, betazoid diaminobenzidine chromogen kits (Biocare Medical) were mixed and added for 10 min or until visible brown color occurred. Slides were rinsed with running tap water, counterstained with hematoxylin for 30 s, and rinsed with tap water. They were then differentiated in 1.5% acid alcohol very briefly, rinsed with tap water, and placed in 0.1% sodium bicarbonate for 10 s. Finally, slides were dehydrated in 95% and 100% ethanol and citrosol solutions and mounted on a coverslip using xylene-based mounting medium.

Imaging

Trichrome and immunohistochemistry staining was imaged using a Zeiss Axiovert 200 light microscope (Zeiss) at 10× magnification for trichrome staining and 40× magnification for immunohistochemistry. Newly formed dermis

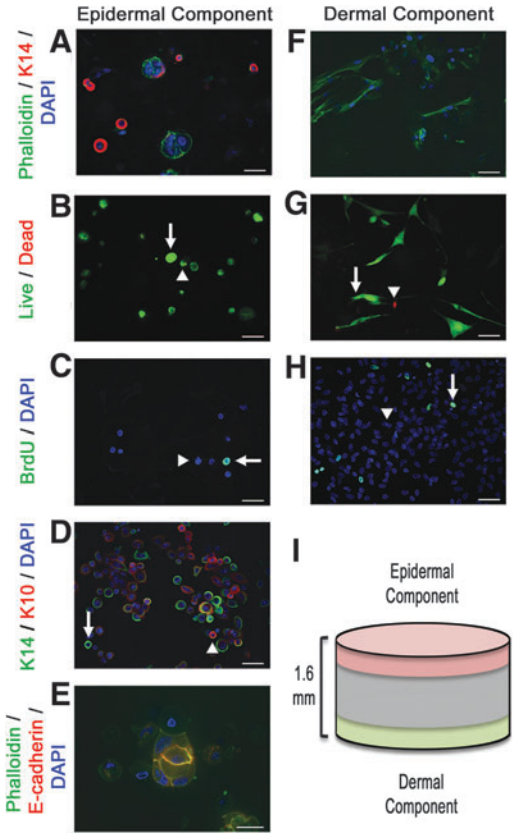

FIG. 3. Cellular characteristics of cellularized PG-1. Images of epidermal component (keratinocytes) and dermal component (fibroblasts) of skin substitute are shown on the *left* side and *right* side respectively. Confocal microscopic images (20× magnification) of **(A)** top and **(F)** bottom of cellularized hydrogels (*green*—phalloidin, *red*—K14, *blue*—DAPI). Images taken 5 days post fibroblast seed and 3 days post keratinocyte seed show clusters of keratinocytes on the top surface of the hydrogel while elongated fibroblasts without keratinocytes are seen on the bottom of the hydrogel. Scale bar represents 50 μm. Live/dead viability (*green*—calcein AM [live cells], *red*—ethidium homodimer-1 [dead cells]) of **(B)** keratinocytes and **(G)** fibroblasts show 92.46% ± 2.26% (mean ± SEM) viable keratinocytes 3 days post seed and 97.74% ± 1.17% (mean ± SEM) viable fibroblasts 5 days post seed. *Arrows* indicate live cells while *arrowheads* indicate dead cells. Images taken at 20× magnification and scale bar represents 50 μm. BrdU proliferation assay (*green*—BrdU, *blue*—DAPI) of **(C)** keratinocytes and **(H)** fibroblasts show 18.27% ± 3.45% (mean ± SEM) BrdU-positive keratinocyte and 3.86% ± 1.42% BrdU-positive fibroblasts. *Arrows* indicate BrdU-positive cells while *arrowheads* indicate BrdU-negative cells. Images taken at 20× magnification and scale bars represent 50 μm. **(D)** Confocal microscopic image of different keratin expression of keratinocytes adhered to pullulan-gelatin hydrogel (*green*—phallodin, *red*—K10, *blue*—DAPI). *Arrows* indicate K14-positive keratinocytes while *arrowheads* indicate K10-positive keratinocytes. Images taken at 20× magnification and scale bars represent 50 μm. **(E)** Confocal microscopic image shows tight clustering of keratinocytes with adherens junction formation (*green*–phalloidin, *red*–e-cadherin, *blue*–DAPI). Image taken at 63× magnification and scale bar represents 20 μm. **(I)** Schematic showing total thickness of hydrogel and areas from which epidermal and dermal component images were taken. BrdU, 5-bromo-2′-deoxyuridine; DAPI, 4′,6-diamidino-2-phenylindole. Color images available online at www.liebertpub.com/tea

''neo-dermis'' thickness was calculated by using three measurements of dermal thickness of wounds taken from trichrome staining imaging. Percentage of F4/80-positive cells, PCNA-positive cells, and of HLA-positive cells were recorded based on immunohistochemistry imaging. Quantification of angiogenesis was performed by counting all vessels as identified with ASM present in the newly formed dermal layer. All quantifications were performed blinded.

Statistical analysis

Statistical comparisons between groups were performed using an ANOVA test followed by unpaired Student's *t* tests if significant differences were observed using Graph Prism software (GraphPad). Two-tailed $p \leq 0.05$ was considered significant. Data were shown with graphs displaying mean of specific group ± SEM.

Results and Discussion

The results of this study show that this novel skin substitute provides both excellent mechanical and cellular characteristics. There was increased wound healing with less inflammatory cell infiltration and increased angiogenesis in cellularized PG-1. The use of a pullulan-collagen hydrogel for wound healing has been accomplished previously,[9,21] yet there are no studies examining the use of pullulan-gelatin hydrogels. As this study used a novel hydrogel composition, it was crucial to investigate its mechanical characteristics since such properties of hydrogels significantly affect their cellular properties.[22–24]

Mechanical characteristics of pullulan-gelatin hydrogel

This study looked at four different mechanical characteristics: porosity, *in vitro* degradation, swelling behavior, and elastic modulus. Porosity refers to the void spaces in a material that provide a route for cell penetration and provide a template for neovascularization. In general, the larger the average pore size, the more cell migration,[25] cell infiltration,[26] extracellular matrix secretion,[27] and increased vascularization.[28] PG-1 had an average pore size of 61.69 ± 2.76 μm (mean ± SEM) with a range of pore sizes from 20 to 200 μm (Fig. 2A). As human dermal fibroblasts have an average diameter of 10–15 μm, they would easily penetrate and adhere throughout the entire porous PG-1. Yet, the larger pore sizes would still allow adequate neovascularization as hydrogels containing these large pores allow mature vascularized tissue formation throughout.[29]

In vitro degradation showed over 50% degradation within 20 min and hydrogels were unable to be weighed effectively after this time point due to significant degradation (Fig. 2B). The rapid *in vitro* degradation of PG-1 when submerged into pullulanase microbial shows that this skin substitute has the potential to be degraded *in vivo*, an important feature of skin substitutes.

Swelling behavior of a skin substitute affects its ability to allow diffusion of nutrients and affects porosity of the skin substitute during the manufacturing process.[30,31] Swelling percentage of PG-1 ranged from 1812% ± 25.46%, 1758% ± 31.74%, and 1801% ± 43.49% (mean ± SEM) when incubated in PBS, fibroblast media, and keratinocyte media respectively, showing almost identical swelling behavior in the different media used in this study (Fig. 2C). The change in size of the hydrogel shows the hydrogel returning back to the original size before freeze-drying. This allows the hydrogel to be cut into a customized shape, stored using a freeze-drying approach, and then easily submerged in a solution to be used clinically.

As skin substitutes develop, there is a further push toward mimicking the elastic properties of human skin for both functional and aesthetic purposes. Increasing a hydrogel's elasticity has the potential to reduce skin contraction clinically.[32] Elastic modulus of the pullulan-gelatin material was 22.43 ± 4.54 kPa (mean ± SEM), which is comparable to

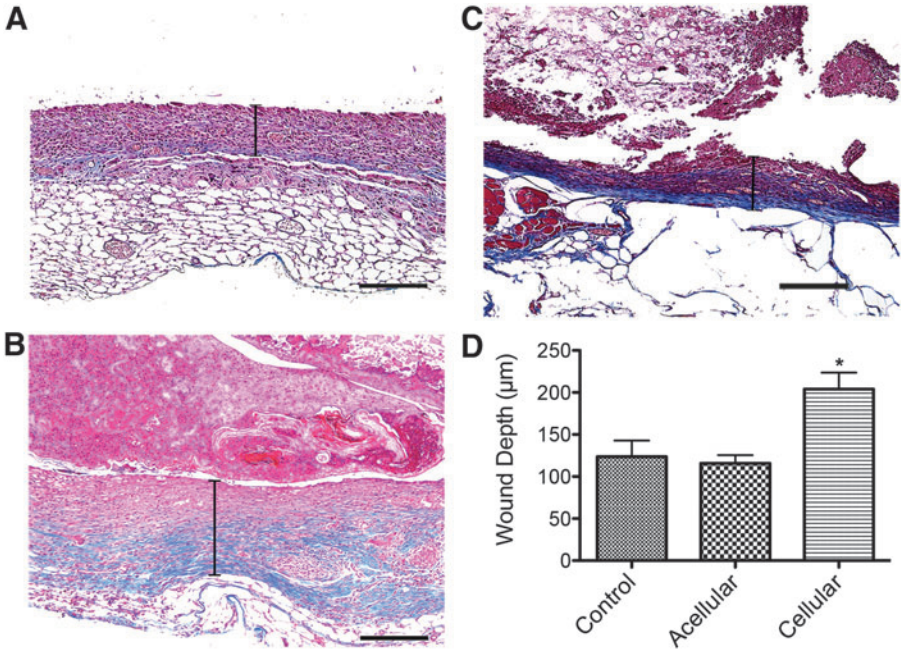

FIG. 4. Cellularized PG-1 significantly increased new skin formation 14 days post punch biopsy compared to acellular hydrogels and control. Representative trichrome-stained images (10× magnification) show new dermal formation 14 days post punch biopsy. Capped bars on images represent dermis thickness (wound depth) in **(A)** control, **(B)** acellular hydrogels, and **(C)** cellular hydrogels. Scale bars represent 200 μm. **(D)** Wound depth was 123.77 ± 21.37 μm, 115.63 ± 9.83 μm, and 204.00 ± 19.65 μm, (mean ± SEM) for control, acellular hydrogels, and cellular hydrogels respectively (*$p < 0.05$). Color images available online at www.liebertpub.com/tea

native human skin (Fig. 2D).[33] Thus, it is hypothesized to experience similar contraction rates as human skin grafts.[34]

Cellular characteristics of cellularized pullulan-gelatin hydrogel

All epidermal component images (Fig. 3A–E) were taken from the top 200 μm of the 1.6 mm thick cellularized hydrogel and all dermal component images were taken from the bottom 200 μm of the hydrogel (Fig. 3F–H) as described in the schematic shown (Fig. 3I). It was not possible to take images past 200 μm into each side of the hydrogels due to limitations of current confocal imaging. Future experiments would include using advanced imaging techniques, such as CLARITY, which has the ability to visualize cells throughout an entire hydrogel.[35]

Clusters of keratinocytes were seen on the top surface of the hydrogel, while the bottom one showed only elongated fibroblasts with bipolar and multipolar morphology (Fig. 3A, F). These differences clearly show that there are two distinct layers in this skin substitute, a feature that has been shown to increase skin regeneration.[15–17] Dermal fibroblasts secrete growth hormones that increase keratinocyte proliferation and promote angiogenesis.[36] Epidermal keratinocytes secrete interleukin-1, a cytokine that not only promotes keratinocyte proliferation and differentiation but also promotes keratinocyte growth factor production from dermal fibroblasts.[36] Keratinocytes also secrete proangiogenic growth factors including vascular endothelial growth factor and platelet-derived growth factor (PDGF).[36] PDGF secretion also plays a secondary role in promoting dermal fibroblast proliferation.[37] These bilayer skin substitutes resemble native skin and promote viability and proliferation of cells better than a single layer skin substitute would.

Looking at cellular viability, live/dead assays show 92.46% ± 2.26% (mean ± SEM) viable keratinocytes 3 days post-seed and 97.74% ± 1.17% (mean ± SEM) viable fibroblasts 5 days post-seed, suggesting that this hydrogel is not toxic to the cells (Fig. 3C, G). To verify the proliferative characteristics of cells adhered onto PG-1, we incubated cells in BrdU-containing media for 24 h before staining for proliferating cells that incorporated BrdU into their nucleus. This BrdU proliferation assay showed 18.27% ± 3.45% (mean ± SEM) BrdU-positive keratinocytes and 3.86% ± 1.42% BrdU-positive fibroblasts, indicating a near ideal cellular microenvironment provided by PG-1 (Fig. 3E, H).

As viability and proliferation are not the only characteristics an ideal skin substitute should have, we sought to ascertain whether cells, particularly keratinocytes, could differentiate while adhered onto the hydrogel. Human skin epidermis is a stratified structure, composed of proliferative basal progenitors that are mainly positive for keratin 14 (K14) and the differentiated cells in spinous layers that express keratin 10 (K10).[38] An ideal hydrogel should provide an environment that not only allows early undifferentiated cells to self-renew, but also allows a subpopulation of them to differentiate, resembling normal skin.

Staining for K10 and K14 showed different expression of keratin on keratinocytes adhered on to PG-1 (Fig. 3G). Staining for e-cadherin, a protein that contributes to adherens junction formation and to the maintenance of epithelial integrity during tissue homeostasis and remodeling,[39] showed clusters of keratinocytes with adherens junction formation on the surface of the hydrogel (Fig. 3H). Adherens junction formation represents advanced stages of epithelialization and shows that PG-1 provides an excellent microenvironment for skin cells *in vitro*.[40]

Cellularized pullulan-gelatin hydrogels enhance wound healing in vivo

Although the mechanical and cellular characteristics of the skin substitute were ideal, the *in vivo* results show the clinical implications for this skin substitute. To evaluate the effect of cellularized PG-1s on skin healing and regeneration, we measured the thickness of newly formed dermis ''neo-dermis'' 14 days post skin biopsy. Neo-dermis thickness was significantly increased ($p < 0.05$) in cellular hydrogels, 204.00 ± 19.65 μm, compared to acellular hydrogels, 115.63 ± 9.83 μm, and controls, 123.77 ± 21.37 μm (mean ± SEM) (Fig. 4). No significant difference was seen between acellular hydrogels

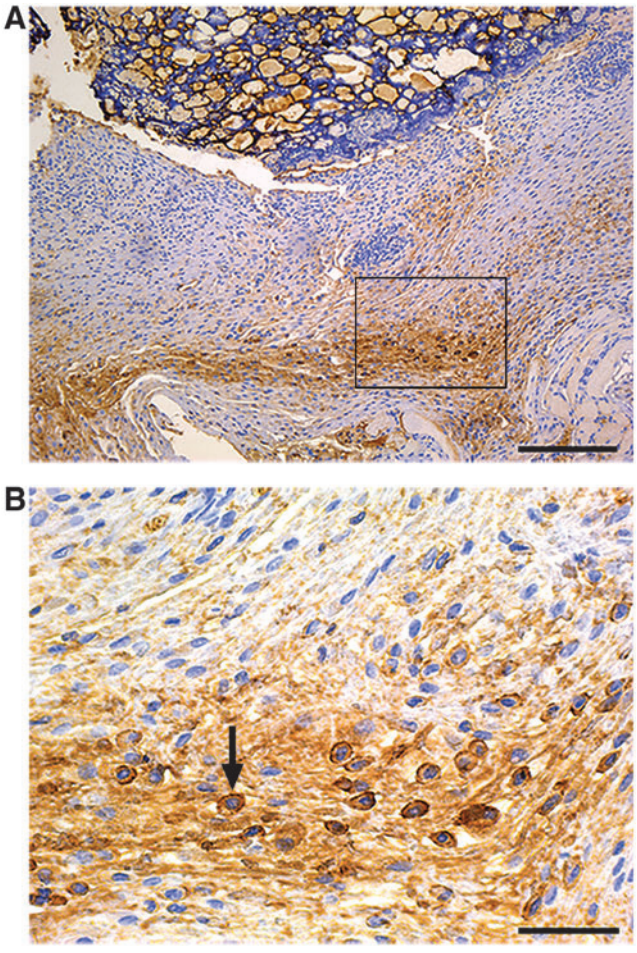

FIG. 5. Human cells were incorporated into newly formed murine dermis 14 days post punch biopsy. Immunohistochemistry staining of HLA showed 4.02% ± 0.78% (mean ± SEM) of skin cells in the murine dermis were HLA-positive cells. **(B)** 40× magnification image of *rectangle* outlined in **(A)** 10× magnification image. *Arrow* indicates HLA-positive cell. Scale bars represent **(A)** 200 μm and **(B)** 50 μm. HLA, human leukocyte antigen. Color images available online at www.liebertpub.com/tea

and controls. This suggests that the incorporation of cells was part of the reason for the enhanced wound healing.

To verify the fate of grafted cells in the newly healed skin, we stained for HLA to visualize human cells. 4.02% ± 0.78% (mean ± SEM) of skin cells in the neodermis treated with cellularized hydrogels were HLA-positive cells, highlighting the successful engraftment of cells sourced from cellularized PG-1s (Fig. 5). This percentage of engrafted cells is similar to previous successful cell engraftment rates using cellularized hydrogels 14 days post skin biopsy.[21]

As previously mentioned, the creation of bilayer skin substitutes creates positive feedback between keratinocytes and fibroblasts to promote viability and proliferation of skin cells.[15–17] It is hypothesized that this positive feedback from the cellularized skin substitute contributed to proliferation of both human cells adhered to the hydrogel and mouse skin cells being recruited to the wound bed. By looking at PCNA, a marker for actively proliferating cells, cellularized hydrogels had significantly increased PCNA-positive cells, 19.03% ± 2.40%, compared to acellular hydrogels, 7.97% ± 2.54%, and controls, 9.93% ± 1.35% (mean ± SEM) (Fig. 6A–D). No significant difference was seen between acellular hydrogels and controls. This provides evidence that as a result of incorporating human cells into PG-1, proliferation of all skin cells in the wound bed increased.

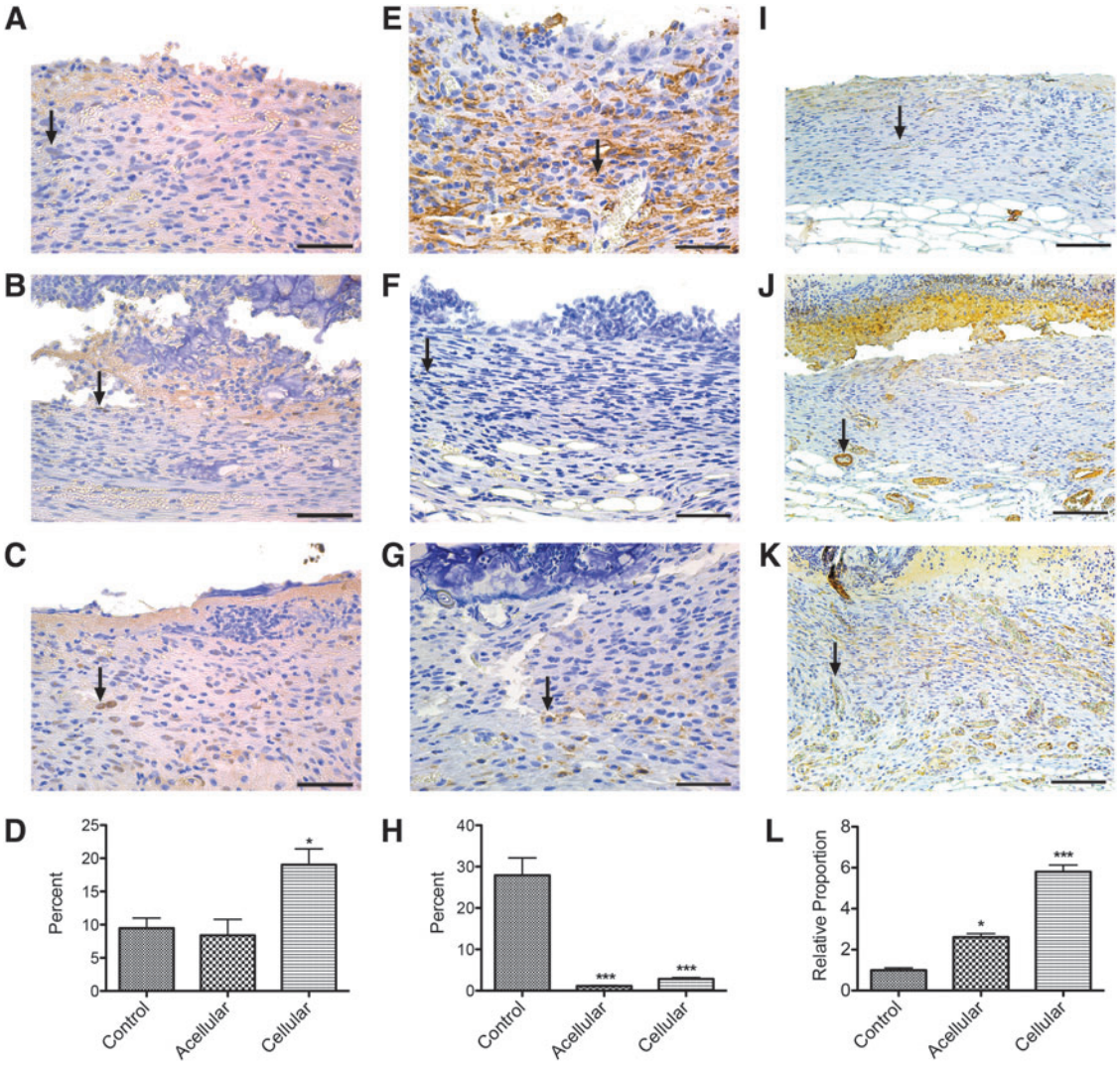

FIG. 6. Cellularized PG-1 increased skin cell proliferation, suppressed excessive immune response, and increased neovascularization. Representative images of immunohistochemistry stained images for **(A–C)** PCNA-positive cells, **(E–G)** F4/80-positive cells, and **(I–K)** ASM-positive cells. *Arrows* indicate cells positive for their respective stains. Scale bars represent 50 μm (40× magnification) for PCNA and F4/80 images and 100 μm (20× magnification) for ASM images. **(D)** Percentage of PCNA-positive cells were 9.93% ± 1.35%, 7.97% ± 2.54%, and 19.03% ± 2.40% (mean ± SEM) for control, acellular hydrogels, and cellular hydrogels respectively. **(H)** Percentage of F4/80-positive cells were 27.94% ± 4.19%, 1.22% ± 0.19%, and 2.84% ± 0.36% (mean ± SEM) for control, acellular hydrogels, and cellular hydrogels respectively. **(L)** Relative proportion of increased number of capillaries found in newly formed dermis was 5.81 ± 0.65 and 2.61 ± 0.34 for cellular hydrogels and acellular hydrogels respectively compared to control (1 ± 0.22) (mean ± SEM) (*$p < 0.05$, ***$p < 0.001$). ASM, alpha-smooth muscle antibody; PCNA, proliferating cell nuclear antigen. Color images available online at www.liebertpub.com/tea

A significant role for macrophages has been shown during skin healing and hypertrophic scar formation.[41–44] While their presence is essential, increased numbers of macrophages lead to hypertrophic scarring, a morbidity that should be avoided. As such, it is important to evaluate whether the hydrogel augments inflammation to avoid unnecessary scarring. Percentage of F4/80-positive cells, a marker of macrophages, was significantly decreased ($p < 0.001$) in acellular hydrogels, $1.22\% \pm 0.19\%$, and cellularized hydrogels, $2.84\% \pm 0.36\%$, compared to controls, $27.94\% \pm 4.19\%$ (mean ± SEM), showing a very promising anti-inflammatory effect of PG-1 (Fig. 6E–H).

Pullulan-based hydrogels have been shown to increase viability of skin cells in high oxidative stress wound beds due to their antioxidant properties.[8] Acute wound injuries have high free radicals due to high levels of infiltrating inflammatory cells, which leads to decreased skin cell viability.[45,46] The neo-dermis after using acellular and cellularized PG-1s in this study showed significantly decreased F4/80-positive cells representing a significant reduction of macrophage infiltration presumably by decreasing free radicals or reactive oxygen species (ROS). Clinically, this skin substitute could be used in chronic skin wounds and burns, injuries with increased ROS, as decreasing inflammation would help improve skin cell viability and skin healing.[47,48]

This decreased inflammation may have also played a role in increased angiogenesis in the neo-dermis. Immunohistochemical staining of alpha-smooth muscle, a marker for vessel walls, showed varying amounts of blood vessels in the dermal layer. The relative proportion of increased number of capillaries found in the neo-dermis was 5.81 ± 0.65 and 2.61 ± 0.34 for cellular hydrogels and acellular hydrogels respectively compared to control (1 ± 0.22) (mean ± SEM) (Fig. 6I–L). Many highly inflammatory chronic skin wounds have altered angiogenesis.[49] Proper angiogenesis is a crucial step toward complete wound healing.[50] Therefore, even with no significant change in dermal thickness between control and acellular hydrogels, the increased vasculature in the wounds treated with acellular hydrogels may indicate further advanced wound healing, possibly related to the decreased inflammation seen 14 days post skin biopsy.

The limitation of our skin substitute is the lack of keratinocytes present in the neo-dermis. Immunohistochemical staining of K10 and K14 (images not shown), markers of keratinocytes, did not show these cells in the healing wound beds. This is partly due to the hydrogel not being fully incorporated at 14 days post skin biopsy. Therefore, the keratinocytes found at the top surface of the hydrogel have not yet integrated in the skin layer. Furthermore, due to the use of domes to prevent mouse skin contracture and the fact that reepithelialization of wounds happens primarily by migrating keratinocytes on the surface of the wound, mouse keratinocytes would not be able to migrate into the wound bed.[40] Future experiments would include increasing the length of time post skin biopsy before excising the wound bed to ensure complete incorporation of the hydrogel into the mouse skin.

Conclusion

PG-1 showed excellent mechanical characteristics for use as a skin substitute. Incorporating both fibroblasts and keratinocytes created a bilayer skin substitute with excellent cell viability, proliferation, differentiation, and morphology. The use of cells to create two distinct layers contributed toward significantly thicker neo-dermis formation with increased numbers of proliferating skin cells 14 days post skin punch biopsy in a mouse model. The use of a pullulan-gelatin hydrogel significantly reduced macrophage infiltration while supporting increased angiogenesis, suggesting that this skin substitute would be ideal in skin wounds with high levels of inflammation, such as burns and chronic skin wounds.[47,48]

Acknowledgments

The authors would like to thank all members of the laboratory, particularly Cassandra Belo, for their assistance throughout the study. This work was supported by Toronto Hydro, Canadian Institutes of Health Research No. 123336, CFI Leader's Opportunity Fund: Project No. 25407, and NIH RO1 GM087285-01.

Disclosure Statement

No competing financial interests exist.

References

1. Shahrokhi, S., Arno, A., and Jeschke, M.G. The use of dermal substitutes in burn surgery: acute phase. Wound Repair Regen **22,** 14, 2014.
2. Greaves, N.S., Iqbal, S.A., Baguneid, M., and Bayat, A. The role of skin substitutes in the management of chronic cutaneous wounds. Wound Repair Regen **21,** 194, 2013.
3. Nyame, T.T., Chiang, H.A., and Orgill, D.P. Clinical applications of skin substitutes. Surg Clin North Am **94,** 839, 2014.
4. Bello, Y.M., Falabella, A.F., and Eaglstein, W.H. Tissue-engineered skin. Current status in wound healing. Am J Clin Dermatol **2,** 305, 2001.
5. Rawlingson, A. Nitric oxide, inflammation and acute burn injury. Burns **29,** 631, 2003.
6. Mogosanu, G.D., and Grumezescu, A.M. Natural and synthetic polymers for wounds and burns dressing. Int J Pharm **463,** 127, 2014.
7. Prajapati, V.D., Jani, G.K., and Khanda, S.M. Pullulan: an exopolysaccharide and its various applications. Carbohydr Polym **95,** 540, 2013.
8. Wong, V.W., Rustad, K.C., Glotzbach, J.P., Sorkin, M., Inayathullah, M., Major, M.R., Longaker, M.T., Rajadas, J., and Gurtner, G.C. Pullulan hydrogels improve mesenchymal stem cell delivery into high-oxidative-stress wounds. Macromol Biosci **11,** 1458, 2011.
9. Wong, V.W., Rustad, K.C., Galvez, M.G., Neofytou, E., Glotzbach, J.P., Januszyk, M., Major, M.R., Sorkin, M., Longaker, M.T., Rajadas, J., and Gurtner, G.C. Engineered pullulan-collagen composite dermal hydrogels improve early cutaneous wound healing. Tissue Eng Part A **17,** 631, 2011.
10. Suzuki, S., Matsuda, K., Isshiki, N., Tamada, Y., and Ikada, Y. Experimental study of a newly developed bilayer artificial skin. Biomaterials **11,** 356, 1990.
11. Jha, B.S., Ayres, C.E., Bowman, J.R., Telemeco, T.A., Sell, S.A., Bowlin, G.L., and Simpson, D.G. Electrospun collagen: a tissue engineering scaffold with unique functional properties in a wide variety of applications. J Nanomater **2011,** 15, 2011.
12. Zhu, J., and Marchant, R.E. Design properties of hydrogel tissue-engineering scaffolds. Expert Rev Med Devices **8,** 607, 2011.

13. Annabi, N., Nichol, J.W., Zhong, X., Ji, C., Koshy, S., Khademhosseini, A., and Dehghani, F. Controlling the porosity and microarchitecture of hydrogels for tissue engineering. Tissue Eng Part B Rev **16,** 371, 2010.
14. Mohd Hilmi, A.B., and Halim, A.S. Vital roles of stem cells and biomaterials in skin tissue engineering. World J Stem Cells **7,** 428, 2015.
15. Spiekstra, S.W., Breetveld, M., Rustemeyer, T., Scheper, R.J., and Gibbs, S. Wound-healing factors secreted by epidermal keratinocytes and dermal fibroblasts in skin substitutes. Wound Repair Regen **15,** 708, 2007.
16. Ghahary, A., and Ghaffari, A. Role of keratinocyte-fibroblast cross-talk in development of hypertrophic scar. Wound Repair Regen **15 Suppl 1,** S46, 2007.
17. Wojtowicz, A.M., Oliveira, S., Carlson, M.W., Zawadzka, A., Rousseau, C.F., and Baksh, D. The importance of both fibroblasts and keratinocytes in a bilayered living cellular construct used in wound healing. Wound Repair Regen **22,** 246, 2014.
18. Aasen, T., and Izpisúa Belmonte, J.C. Isolation and cultivation of human keratinocytes from skin or plucked hair for the generation of induced pluripotent stem cells. Nat Protoc **5,** 371, 2010.
19. Frank, D.E., and Carter, W.G. Laminin 5 deposition regulates keratinocyte polarization and persistent migration. J Cell Sci **117,** 1351, 2004.
20. Garg, R.K., Rennet, R.C., Duscher, D., Sorkin M., Kosaraju R., Auerbach LJ., Lennon J., Chung, M.T., Paik, K., Nimpf, J., Rajadas, J., Longaker, M.K., and Gurtner G.C. Capillary force seeding of hydrogels for adipose-derived stem cell delivery in wounds. Stem Cells Trans Med **3,** 1079, 2014.
21. Rustad, K.C., Wong, V.W., Sorkin, M., Glotzbach, J.P., Major, M.R., Rajadas, J., Longaker, M.T., and Gurtner, G.C. Enhancement of mesenchymal stem cell angiogenic capacity and stemness by a biomimetic hydrogel scaffold. Biomaterials **33,** 80, 2012.
22. Lee, M., Wu, B.M., and Dunn, J.C. Effect of scaffold architecture and pore size on smooth muscle cell growth. J Biomed Mater Res A **87,** 1010, 2008.
23. Murphy, C.M., and O'Brien, F.J. Understanding the effect of mean pore size on cell activity in collagen-glycosaminoglycan scaffolds. Cell Adh Migr **4,** 377, 2010.
24. Howard, D., Buttery, L.D., Shakesheff, K.M., and Roberts, S.J. Tissue engineering: strategies, stem cells and scaffolds. J Anat **213,** 66, 2008.
25. Sunami, H., Yokota, I., and Igarashi, Y. Influence of the pattern size of micropatterned scaffolds on cell morphology, proliferation, migration and F-actin expression. Biomater Sci **2,** 399, 2014.
26. Phipps, M.C., Clem, W.C., Grunda, J.M., Clines, G.A., and Bellis, S.L. Increasing the pore sizes of bone-mimetic electrospun scaffolds comprised of polycaprolactone, collagen I and hydroxyapatite to enhance cell infiltration. Biomaterials **33,** 524, 2012.
27. Lien, S.M., Ko, L.Y., and Huang, T.J. Effect of pore size on ECM secretion and cell growth in gelatin scaffold for articular cartilage tissue engineering. Acta biomater **5,** 670, 2009.
28. Joshi, V.S., Lei, N.Y., Walthers, C.M., Wu, B., and Dunn, J.C. Macroporosity enhances vascularization of electrospun scaffolds. J Surg Res **183,** 18, 2013.
29. Chiu, Y.C., Cheng, M.H., Engel, H., Kao, S.W., Larson, J.C., Gupta, S., and Brey, E.M. The role of pore size on vascularization and tissue remodeling in PEG hydrogels. Biomaterials **32,** 6045, 2011.
30. Pan, J.-F., Liu, N.-H., Sun, H., and Xu, F. Preparation and characterization of electrospun PLCL/poloxamer nanofibers and dextran/gelatin hydrogels for skin tissue engineering. PLoS One **9,** e112885, 2014.
31. Kang, H.-W., Tabata, Y., and Ikada, Y. Fabrication of porous gelatin scaffolds for tissue engineering. Biomaterials **20,** 1339, 1999.
32. Rnjak, J., Wise, S.G., Mithieux, S.M., and Weiss, A.S. Severe burn injuries and the role of elastin in the design of dermal substitutes. Tissue Eng Part B Rev **17,** 81, 2011.
33. Xing, L., and Boppart, S.A. Biomechanical properties of in vivo human skin from dynamic optical coherence elastography. IEEE Trans Biomed Eng **57,** 953, 2010.
34. Fritz, J.R., Phillips, B.T., Conkling, N., Fourman, M., Melendez, M.M., Bhatnagar, D., Simon, M., Rafailovich, M., and Dagum, A.B. Comparison of native porcine skin and a dermal substitute using tensiometry and digital image speckle correlation. Ann Plast Surg **69,** 462, 2012.
35. Tomer, R., Ye, L., Hsueh, B., and Deisseroth, K. Advanced CLARITY for rapid and high-resolution imaging of intact tissues. Nat Protoc **9,** 1682, 2014.
36. Maas-Szabowski, N., Szabowski, A., Stark, H.J., Andrecht, S., Kolbus, A., Schorpp-Kistner, M., Angel, P., and Fusenig, N.E. Organotypic cocultures with genetically modified mouse fibroblasts as a tool to dissect molecular mechanisms regulating keratinocyte growth and differentiation. J Invest Dermatol **116,** 816, 2001.
37. Barrientos, S., Stojadinovic, O., Golinko, M.S., Brem, H., and Tomic-Canic, M. Growth factors and cytokines in wound healing. Wound Repair Regen **16,** 585, 2008.
38. Hsu, Y.C., Li, L., and Fuchs, E. Emerging interactions between skin stem cells and their niches. Nat Med **20,** 847, 2014.
39. Baum, B., and Georgiou, M. Dynamics of adherens junctions in epithelial establishment, maintenance, and remodeling. J Cell Biol **192,** 907, 2011.
40. Pastar, I., Stojadinovic, O., Yin, N.C., Ramirez, H., Nusbaum, A.G., Sawaya, A., Patel, S.B., Khalid, L., Isseroff, R.R., and Tomic-Canic, M. Epithelialization in wound healing: a comprehensive review. Adv Wound Care **3,** 445, 2014.
41. Bielefeld, K.A., Amini-Nik, S., Whetstone, H., Poon, R., Youn, A., Wang, J., and Alman, B.A. Fibronectin and beta-catenin act in a regulatory loop in dermal fibroblasts to modulate cutaneous healing. World J Biol Chem **286,** 27687, 2011.
42. Bielefeld, K.A., Amini-Nik, S., and Alman, B.A. Cutaneous wound healing: recruiting developmental pathways for regeneration. Cell Mol Life Sci **70,** 2059, 2013.
43. Amini-Nik, S., Glancy, D., Boimer, C., Whetstone, H., Keller, C., and Alman, B.A. Pax7 expressing cells contribute to dermal wound repair, regulating scar size through a beta-catenin mediated process. Stem Cells **29,** 1371, 2011.
44. Amini-Nik, S., Cambridge, E., Yu, W., Guo, A., Whetstone, H., Nadesan, P., Poon, R., Hinz, B., and Alman, B.A. beta-Catenin-regulated myeloid cell adhesion and migration determine wound healing. J Clin Invest **124,** 2599, 2014.
45. Gurtner, G.C., Werner, S., Barrandon, Y., and Longaker, M.T. Wound repair and regeneration. Nature **453,** 314, 2008.

46. Pasparakis, M., Haase, I., and Nestle, F.O. Mechanisms regulating skin immunity and inflammation. Nat Rev Immunol **14,** 289, 2014.
47. Telgenhoff, D., and Shroot, B. Cellular senescence mechanisms in chronic wound healing. Cell Death Differ **12,** 695, 2005.
48. Parihar, A., Parihar, M.S., Milner, S., and Bhat, S. Oxidative stress and anti-oxidative mobilization in burn injury. Burns **34,** 6, 2008.
49. Varricchi, G., Granata, F., Loffredo, S., Genovese, A., and Marone, G. Angiogenesis and lymphangiogenesis in inflammatory skin disorders. J Am Acad Dermatol **73,** 144, 2015.
50. Tonnesen, M.G., Feng, X., and Clark, R.A. Angiogenesis in wound healing. J Invest Dermatol **5,** 40, 2000.

Address correspondence to:
Saeid Amini-Nik, MSc, MD, PhD
Department of Surgery
Sunnybrook Research Institute
Ross Tilley Burn Centre
University of Toronto
Room: M7-140, 2075 Bayview Avenue
Toronto M4N 3 M5
Ontario
Canada

E-mail: saeid.amininik@utoronto.ca

Received: November 30, 2015
Accepted: April 12, 2016
Online Publication Date: May 5, 2016